Antonino Morassi
Fabrizio Vestroni
Editors

International Centre
for Mechanical Sciences

Dynamic Methods for Damage Detection in Structures

CISM Courses and Lectures, vol. 499

SpringerWienNewYork

SpringerWienNewYork

CISM COURSES AND LECTURES

The series presents lecture notes, monographs, edited works and proceedings in the field of Mechanics, Engineering, Computer Science and Applied Mathematics.
Purpose of the series is to make known in the international scientific and technical community results obtained in some of the activities organized by CISM, the International Centre for Mechanical Sciences.

INTERNATIONAL CENTRE FOR MECHANICAL SCIENCES

COURSES AND LECTURES - No. 499

DYNAMIC METHODS FOR DAMAGE DETECTION IN STRUCTURES

EDITED BY

ANTONINO MORASSI
UNIVERSITY OF UDINE, ITALY

FABRIZIO VESTRONI
UNIVERSITY OF ROMA LA SAPIENZA, ITALY

SpringerWienNewYork

This volume contains 108 illustrations

Printed in Italy
SPIN 12244355

All contributions have been typeset by the authors.

ISBN 978-3-211-78776-2 SpringerWienNewYork

PREFACE

Non-destructive testing aimed at monitoring, structural identification and diagnostics is of strategic importance in many branches of civil and mechanical engineering. This type of tests is widely practiced and directly affects topical issues regarding the design of new buildings and the repair and monitoring of existing ones. The load-bearing capacity of a structure can now be evaluated using well-established mechanical modelling methods aided by computing facilities of great capability. However, to ensure reliable results, models must be calibrated with accurate information on the characteristics of materials and structural components. To this end, non-destructive techniques are a useful tool from several points of view. Particularly, by measuring structural response, they provide guidance on the validation of structural descriptions or of the mathematical models of material behaviour.

Diagnostic engineering is a crucial area for the application of non-destructive testing methods. Repeated tests over time can indicate the emergence of possible damage occurring during the structure's lifetime and provide quantitative estimates of the level of residual safety.

Of the many non-destructive testing techniques now available, dynamic methods enjoy growing focus among the engineering community. Conventional diagnostic methods, such as those based on visual inspection, thermal or ultrasonic analysis, are local by nature. To be effective these require direct accessibility of the region to be inspected and a good preliminary knowledge of the position of the defective area. Techniques based on the study of the dynamic response of the structure or wave propagation, on the contrary, are a potentially effective diagnostic tool. These can operate on a global scale and do not require a priori information on the damaged area.

Recent technological progress has generated extremely accurate and reliable experimental methods, enabling a good estimate of changes in the dynamic behaviour of a structural system caused by possible damage. Although experimental techniques are now well-established, the interpretation of measurements still lags somewhat behind. This particularly concerns identification and structural diagnostics due to their nature of inverse problems. Indeed, in these applications one wishes to determine some mechanical properties of a system on the basis of measurements of its response, in part exchanging the role of the unknowns and data compared to the direct problems of structural analysis.

Hence, concerns typical of inverse problems arise, such as high nonlinearity, non-uniqueness or non-continuous dependence of the solution on the data. When identification techniques are applied to the study of real-world structures,

additional obstacles arise given the complexity of structural modelling, the inaccuracy of the analytical models used to interpret experiments, measurement errors and incomplete field data. Furthermore, the results of the theoretical mathematical formulation of problems of identification and diagnostics, given the present state-of-knowledge in the field, focus on quality, while practical needs often require more specific and quantitative estimates of quantities to be identified. To overcome these obstacles, standard procedures often do not suffice and an individual approach must be applied to tackle the intrinsic nature of the problem, using specific experimental, theoretical and numerical methods. It is for these reasons that use of damage identification techniques still involves delicate issues that are only now being clarified in international scientific literature.

The CISM Course "Dynamic Methods for Damage Detection in Structures" was an opportunity to present an updated state-of-the-art overview. The aim was to tackle both theoretical and experimental aspects of dynamic non-destructive methods, with special emphasis on advanced research in the field today.

The opening chapter by Vestroni and Pau describes basic concepts for the dynamic characterization of discrete vibrating systems. Chapter 2, by Friswell, gives an overview of the use of inverse methods in damage detection and location, using measured vibration data. Regularisation techniques to reduce ill-conditioning effects are presented and problems discussed relating to the inverse approach to structural health monitoring, such as modelling errors, environmental effects, damage models and sensor validation. Chapter 3, by Betti, presents a methodology to identify mass, stiffness and damping coefficients of a discrete vibrating system based on the measurement of input/output time histories. Using this approach, structural damage can be assessed by comparing the undamaged and damaged estimates of the physical parameters. Cases of partial/limited instrumentation and the effect of model reduction are also discussed. Chapter 4, by Vestroni, deals with the analysis of structural identification techniques based on parametric models. A numerical code, that implements a variational procedure for the identification of linear finite element models based on modal quantities, is presented and applied for modal updating and damage detection purposes. Pseudo-experimental and experimental cases are solved. Ill-conditioning and other peculiarities of the method are also investigated. Chapter 5, by Vestroni, deals with damage detection in beam structures via natural frequency measurements. Cases of single, multiple and interacting cracks are considered in detail. Attention is particularly focussed on the consequences that certain peculiarities, such as the limited number of unknowns (e.g., locations and stiffness reduction of damaged sections), have on the inverse problem solution. The analysis of damage identification in vibrating beams is continued in Chapter 6 by Morassi. Damage analysis

is formulated as a reconstruction problem and it is shown that frequency shifts caused by damage contain information on certain Fourier coefficients of the unknown stiffness variation. The rest of the chapter is devoted to the identification of localized damage in beams from a minimal set of natural frequency measurements. Closed form solutions for certain crack identification problems in vibrating rods and beams are presented. Applications based on changes in the nodes of the mode shapes and on antiresonant data are also discussed. Chapter 7, by Testa, is on the localization of concentrated damage in beam structures based on frequency changes caused by the damage. A second application deals with a crack closure that may develop in fatigue and the potential impact on damage detection. Chapter 8 proposes a paper by Cawley on the use of guided waves for long-range inspection and the integrity assessment of pipes. The aim is to determine the reflection coefficients from cracks and notches of varying depth, circumferential and axial extent when the fundamental torsional mode is travelling in the pipe. Chapter 9, by Vestroni and Vidoli, discusses a technique to enhance sensitivity of the dynamic response to local variations of the mechanical characteristics of a vibrating system based on coupling with an auxiliary system. An application to a beam-like structure coupled to a network of piezoelectric patches is discussed in detail to illustrate the approach.

Antonino Morassi
Fabrizio Vestroni

CONTENTS

Elements of Experimental Modal Analysis

Fabrizio Vestroni* and Annamaria Pau*

* Dipartimento di Ingegneria Strutturale e Geotecnica, University of Roma *La Sapienza*, Italy

Abstract Fundamental concepts for the characterization of the dynamical response of SDOF and NDOF systems are provided. A description is given of the main techniques to represent the response in the frequency domain and its experimental characterization. Two classical procedures of modal parameter identification are outlined and selected numerical and experimental examples are reported.

1 Dynamic Characterization of a SDOF

The experimental study of a structure provides an insight into the real behavior of the system. In particular, the study of its dynamic response, exploiting vibration phenomena, aims to determine the dynamic properties closely connected to the geometrical and mechanical characteristics of the system. Hence, some concepts of structural dynamics will be briefly summarized. It is assumed that the reader has had some exposure to the matter (Craig, 1981; Meirovitch, 1997; Ewins, 2000; Braun et al., 2001).

The classical model of a single degree-of-freedom (SDOF) system is the spring-mass-dashpot model of Figure 1, where the equation of motion and the steady-state solution is reported. Assuming a harmonic excitation, the frequency response function (FRF) $H(\omega)$ can be defined as the ratio between the amplitude of the steady-state response and the load intensity. The FRF shows that in a small range of the ratio ω/ω_0, when the frequency of the excitation approaches the natural frequency of the system, the response amplitude is much larger than the static response. This is called resonance. Furthermore, the amplitude of the steady-state response is linearly dependent on both p_0 and $H(\omega)$. By knowing $H(\omega)$ the response of a SDOF system to a harmonic excitation can be estimated.

In the real world, forces are not simply harmonic, being frequently periodic or approximated closely by periodic forces. A periodic function $p(t)$ having period T_1 can be represented as a series of harmonic components by means of its Fourier series expansion. As an example, in Figure 2, the Fourier series expansion is applied to a square wave. The Fourier series is convergent, i.e. the more terms used, the better the approximation obtained.

Since the response of a SDOF system to a harmonic force is known and a periodic forcing function $p(t)$ can be represented as a sum of harmonic forces, the response of the system $u(t)$ to a periodic excitation can be obtained by exploiting the principle of effect superposition:

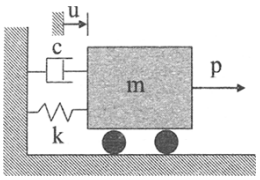

equation of motion

$$m\ddot{u} + c\dot{u} + ku = p_0 \sin(\omega_1 t)$$

steady state response

$$u(t) = p_0 H(\omega) \sin(\omega_1 t - \alpha)$$

$$\tan(\alpha) = \frac{2\zeta\omega/\omega_0}{1-(\omega/\omega_0)^2}$$

$$H(\omega) = \frac{1/k}{\sqrt{1-\left(\frac{\omega}{\omega_0}\right)^2 + 2\zeta\left(\frac{\omega}{\omega_0}\right)^2}}$$

harmonic excitation

$$p(t) = p_0 \cos(\omega_1 t) \quad \text{or} \quad p(t) = p_0 \sin(\omega_1 t)$$

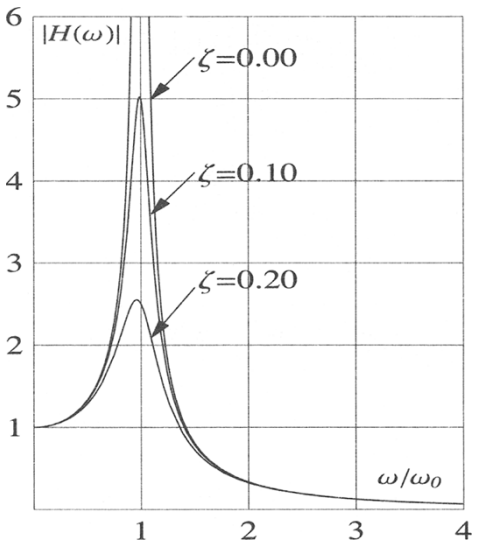

Figure 1. Response of a SDOF system to a harmonic excitation.

$$p(t) = \sum_{n=1}^{\infty} p_n \cos(\omega_n t + \varphi_n), \quad \omega_n = n\omega_1 \tag{1.1}$$

$$u(t) = \sum_{n=1}^{\infty} U_n \cos(\omega_n t + \varphi_n - \alpha_n) \tag{1.2}$$

$$U_n = \frac{p_n/k}{\sqrt{(1-r_n^2)^2 + (2\zeta r_n)^2}} = p_n H(\omega_n, \zeta), \quad tg\alpha_n = \frac{2\zeta r_n}{1-r_n^2}, \quad r_n = \frac{\omega_n}{\omega_0}. \tag{1.3}$$

In this case, too, a knowledge of $H(\omega)$ is sufficient to predict the response of the system.

The steady-state response of a SDOF system to a harmonic force can also be written in complex form, where the bar denotes complex quantities:

$$\overline{u}(t) = \overline{U}(\omega) e^{i\omega t} = \overline{H}(\omega) p_0 e^{i\omega t} \quad \text{and} \quad \overline{H}(\omega) = \frac{1/k}{\left[1-(r)^2\right] + i(2\zeta r)}. \tag{1.4}$$

It is clear that the amplitude and phase of the steady-state response are determined from the amplitude and phase of the complex FRF.

$$\text{periodic excitation} \quad T_1, \omega_1 \quad p(t) = a_0 + \sum_{n=1}^{\infty} a_n \cos(n\omega_1 t) + \sum_{n=1}^{\infty} b_n \sin(n\omega_1 t)$$

$$\text{example: square wave} \quad T_1 = 1 \quad p(t) = \sum_{n=1,3}^{\infty} b_n \sin(n\omega_1 t) \quad \text{odd function}$$

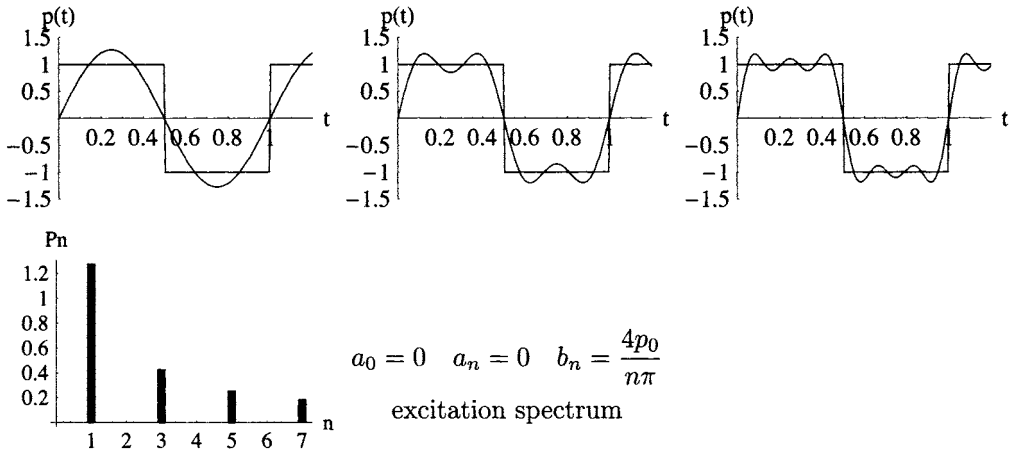

Figure 2. Fourier series expansion of a square wave.

If the forcing function is periodic, the response can be written as:

$$\overline{u}(t) = \sum_{n=-\infty}^{\infty} \overline{U}_n \, e^{in\omega t} = \sum_{n=-\infty}^{\infty} \overline{H}(\omega_n) \, \overline{p}_n \, e^{in\omega t}. \tag{1.5}$$

When the excitation is non periodic, it can be represented by a Fourier integral, which is obtained from the Fourier series by letting the period T_1 approach infinity. Let us define:

$$T_1 = \frac{2\pi}{\omega_1}, \quad \omega_1 = \Delta\omega, \quad n\omega_1 = \omega_n. \tag{1.6}$$

In the Fourier series

$$p(t) = \sum_{n=-\infty}^{\infty} \overline{p}_n(\omega_n) \, e^{i\omega_n t}, \quad \overline{p}_n(\omega_n) = \frac{1}{T_1} \int_{T_1} p(t) \, e^{-i\omega_n t} dt \tag{1.7}$$

since T_1 tends to infinity, p_n is newly defined as:

$$\overline{p}_n(\omega_n) = T_1 \overline{p}_n(\omega_n) \quad \text{and} \quad p(t) = \sum_{n=-\infty}^{\infty} \frac{\Delta\omega}{2\pi} \overline{p}_n(\omega_n) \, e^{in\Delta\omega t}. \tag{1.8}$$

When $T_1 \longrightarrow \infty$, $n\Delta\omega = \omega_n = \omega$ becomes a continuous variable and $\Delta\omega$ becomes the differential $d\omega$, then a Fourier transform pair is obtained:

$$\bar{P}(\omega) = \int_{-\infty}^{\infty} p(t) e^{-i\omega t} dt \quad \text{direct Fourier transform} \tag{1.9}$$

$$p(t) = \int_{-\infty}^{\infty} \frac{1}{2\pi} \overline{P}(\omega) e^{i\omega t} d\omega \quad \text{inverse Fourier transform.} \tag{1.10}$$

When the forcing function is non periodic, a relationship in the frequency domain between the response and the force can be obtained by applying the Fourier transform to each term of the motion equation:

$$\left(-m\omega^2 + ic\omega + k\right) \bar{U}(\omega) = \bar{P}(\omega) \tag{1.11}$$

where use is made of the following properties:

$$\dot{\bar{U}}(\omega) = \frac{i\omega}{2\pi} \int_{-\infty}^{\infty} u(t) e^{-i2\pi ft} dt = \frac{i\omega}{2\pi} \bar{U}(\omega) \tag{1.12}$$

$$\ddot{\bar{U}}(\omega) = \frac{-\omega^2}{2\pi} \int_{-\infty}^{\infty} u(t) e^{-i2\pi ft} dt = \frac{-\omega^2}{2\pi} \bar{U}(\omega). \tag{1.13}$$

The Fourier transform of the response is obtained as the product of the complex FRF and the Fourier transform of the excitation

$$\bar{U}(\omega) = \bar{H}(\omega) \bar{P}(\omega). \tag{1.14}$$

Once $U(\omega)$ is known, the response in the time domain is given by the inverse Fourier transform:

$$\overline{u}(t) = \int_{-\infty}^{\infty} \frac{1}{2\pi} \overline{U}(\omega) e^{i2\pi ft} df. \tag{1.15}$$

In this case also, by knowing $H(\omega)$, the response to a generic excitation can be estimated.

A significant relationship exists between the $H(\omega)$ and the unit impulse response $h(t)$. The latter defines the SDOF response in the time domain to a forcing function equal to a Dirac delta. Since the Fourier transform of an impulse $p(t)=\delta(0)$ is

$$p(\omega) = \frac{1}{2\pi}, \tag{1.16}$$

the impulse response can be written as

$$u(t) = h(t) = \int_{-\infty}^{\infty} \overline{H}(\omega) \overline{p}(\omega) e^{i\omega t} d\omega = \frac{1}{2\pi} \int_{-\infty}^{\infty} \overline{H}(\omega) e^{i\omega t} d\omega. \tag{1.17}$$

In other words, the time domain response to a Dirac delta is the inverse Fourier transform of the FRF. The FRF and the impulse response function form a couple of Fourier transforms. It is possible to refer both to $H(\omega)$ or to $h(t)$ to characterize the system and to provide a predictive model.

2 Display of a FRF

As a complex quantity, the FRF contains information regarding both the amplitude and the phase of the oscillation.

The real and imaginary components of $H(\omega)$ are:

$$H_R(\omega) = \frac{(1-r^2)/k}{(1-r^2)^2 + (2\zeta r)^2} \quad H_I(\omega) = \frac{-2\zeta r/k}{(1-r^2)^2 + (2\zeta r)^2}. \tag{2.1}$$

The three most common forms of representation of $H(\omega)$ are reported in Figure 3-4 for a SDOF with $\zeta = 0.125$.

(1) Real and Imaginary parts of $H(\omega)$ vs r (Figure 3). The real part of $H(\omega)$ crosses the frequency axis at resonance, while, at the same frequency, the imaginary part reaches a minimum.

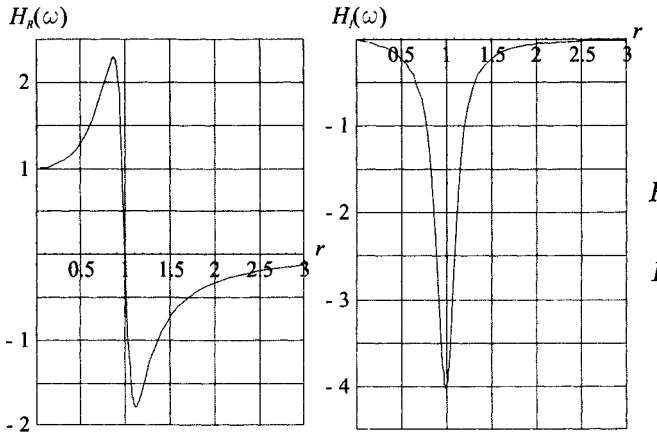

$$H_R(\omega) = \frac{1-r^2/k}{(1-r^2)^2 + (2\zeta r)^2}$$

$$H_I(\omega) = \frac{-2\zeta r/k}{(1-r^2)^2 + (2\zeta r)^2}$$

Figure 3. Real and Imaginary part of the FRF vs r.

(2) Modulus of FRF and phase vs r (Figure 4). Resonance is pointed out by a maximum in the modulus of the FRF and by a phase change from 0 to -π.

(3) Real part vs Imaginary part in the Argand plane (Figure 4). This is a circular loop that contains all the information and enhances the region close to resonance, which is practically coincident with the intersection of the circle with the y axis.

The dynamic properties of a system can be expressed in terms of any convenient response characteristics: FRF can be presented in terms of displacement (receptance), velocity (mobility) or acceleration (intertance). Mobility and inertance are obtained from receptance by multiplying by $i\omega$ and $(i\omega)^2$, respectively.

From the analytical relationships, previously reported, it is clear that the FRF can be experimentally evaluated mainly by two different methods (Ewins, 2000; Maia and Silva, 1997). The former involves the steady-state response to a harmonic force P at different assigned frequencies, which implies the use of an exciter connected to the structure that

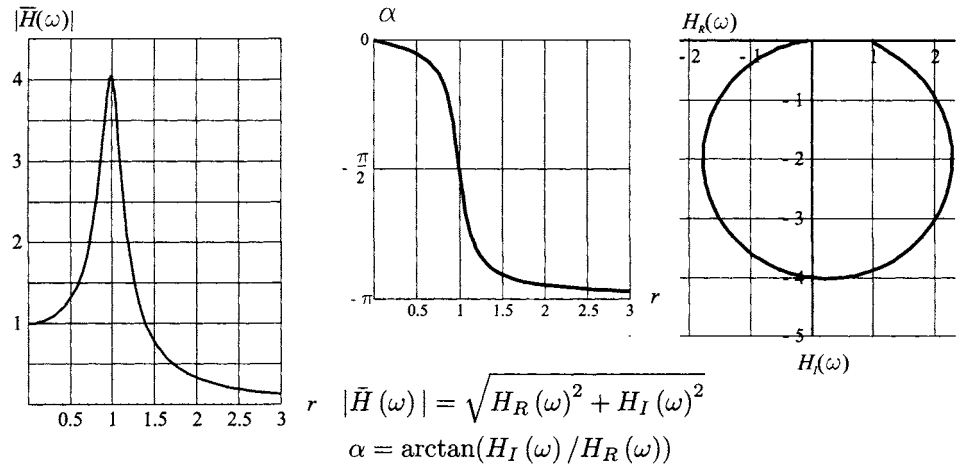

Figure 4. Modulus of FRF and phase vs r and Argand plane.

generates a harmonic force. The amplitude U of the stationary response is recorded and the values of the FRF at the discrete frequencies ω_j of the applied force are directly obtained from the ratio:

$$H(\omega_j) = \frac{U}{P}. \tag{2.2}$$

The other method involves free oscillations of the structure and includes devices which are able to exert impulsive force, such as an instrumented hammer or a sharp release of a static force. The FRF is obtained as the ratio between the response Fourier transform and the input Fourier transform:

$$H(\omega) = \frac{U(\omega)}{P(\omega)}. \tag{2.3}$$

Through this relationship, $H(\omega)$ can only be obtained in the frequency band contained in the forcing function. In particular, the input generated by a real impulsive force has a wide spectrum which is flat within a frequency band $0 - f_{max}$, then rapidly approaches zero. This implies that f_{max} is not infinite, as in the theoretical Dirac delta, but that in the real world depends on the impulse duration T.

In the example of Figure 5, the duration of an experimental impulse is about 0.0006s and the related Fourier transform is constant only up to about 1000 Hz, then rapidly decreases and reaches zero at 3000 Hz, which can be approximately estimated as $2/T$.

3 Dynamic Characterization of Multidegree-of-Freedom Systems

The multidegree-of-freedom systems are representative of discrete systems or discretized continuous systems. The governing equations of motion of a linear system with N-degrees-of-freedom (NDOF) can be written in matrix form as (Craig, 1981; Meirovitch, 1997)

$$\mathbf{M}\,\ddot{u}(t) + \mathbf{C}\,\dot{u}(t) + \mathbf{K}\,u(t) = p(t) \tag{3.1}$$

where $\mathbf{M}$, $\mathbf{C}$ and $\mathbf{K}$ are respectively the mass, damping and stiffness matrices, with dimensions $N \times N$ and $p(t)$ is the force vector. If the damping matrix $\mathbf{C}$ is proportional

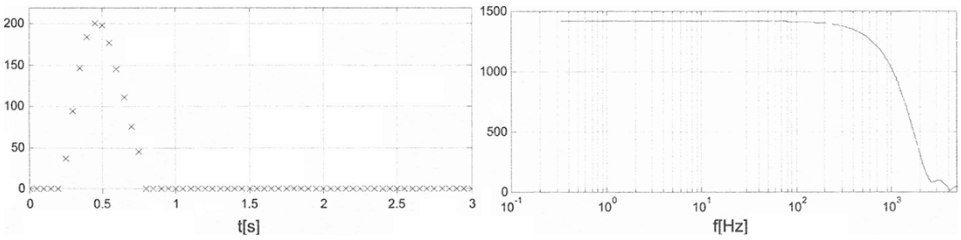

Figure 5. Experimental impulse (left) and its Fourier transform (right).

to a linear combination of $\mathbf{M}$ and $\mathbf{K}$, the damped system will have real eigenvectors coincident with that of the undamped system (classical damping), so that the equations of motion can be decoupled by describing the displacement motion in terms of eigenvectors weighted by the modal coordinates $q(t)$

$$u(t) = \Phi q(t) = \sum_r \Phi_r q_r(t). \tag{3.2}$$

By substituting this expression in the equations of motion, then pre-multiplying by the matrix Φ^T and using the orthogonality eigenvector conditions, N uncoupled modal equations are obtained:

$$\ddot{q}_r(t) + 2\zeta_r \omega_r \dot{q}_r(t) + k_r q_r(t) = p_r(t) \qquad r = 1, N. \tag{3.3}$$

Hence, the system behaviour is represented as a linear superposition of the response of N SDOF systems. In this case, the FRF is a matrix $N \times N$; the displacement in the node i caused by a force applied in node j is:

$$H_{ij}(\omega) = \sum_{r=1}^{N} \frac{\Phi_{ir}\Phi_{jr}}{k_r\left[(1 - r_r^2) + i2\zeta_r r_r\right]}. \tag{3.4}$$

An NDOF systems has N natural frequencies ω_r and N related mode shapes Φ_r along with the modal damping coefficients ζ_r. These are the dynamic characteristics of the structure. When the structure is excited by a harmonic force with a frequency coincident to one of its natural frequencies, the response is amplified. As an example, Figure 6 reports the modulus of $H_{33}(\omega)$ and the mode shapes of a 3DOF shear-type frame. The FRF exhibits three sharp peaks at natural frequencies ω_1, ω_2, ω_3. H_{13}, H_{23}, H_{33} may be obtained by the response measured at nodes 1, 2 and 3 to a forcing function applied in the node 3.

With regard to a 3DOF system, Figure 7 reports H_{11} and H_{21}, represented in two of the three possible forms described for a SDOF system. From these curves, the resonances can be obtained as for the SDOF system, as well as other data needed to define the mode shapes. When dealing with a NDOF system, it is mandatory to define if two points oscillate in phase. The difference of phase between two points in a mode can be directly read from the phase plot. As an example, nodes 1 and 2 oscillate in-phase in mode 1 and

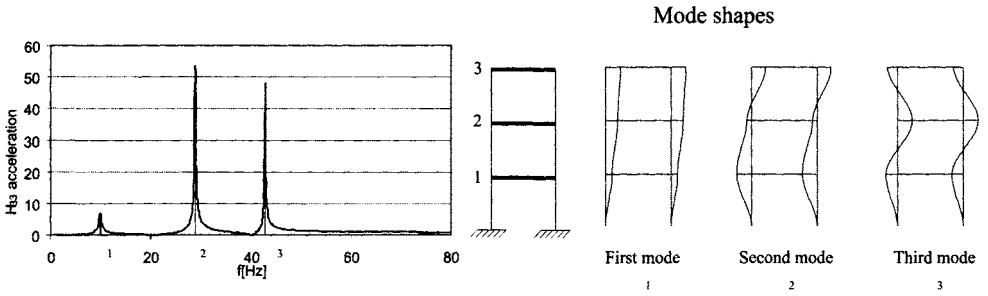

Figure 6. FRF and mode shapes of a 3DOF shear-type frame.

2. In fact, the phase difference between the two responses is zero. By contrast, these two nodes oscillate out-of-phase in mode 3, as shown by a π phase difference. The information can also be deduced from the Nyquist plot: a change in the quadrant occupied by the circles pinpoints a π phase difference. This is indicated in Figure 7 for the third mode. The results are in agreement with the mode shapes of Figure 7.

Figure 8 shows the Fourier transform of acceleration response of a simply supported continuous beam measured in CH2 obtained by means of a static force in CH3 sharply removed (left) or of a hammer impulse (right) at the same point. As for the NDOF, each peak corresponds to a natural frequency. The impulsive force is more effective in exciting a large number of frequencies with respect to the imposed initial displacement.

4 Modal Parameter Identification

Once the registration of the response is available, there are various procedures in the time domain and in the frequency domain to determine the modal properties of the structure. Two classical procedures are presented here. The first algorithm presented is based on a multimodal estimate in the frequency domain, following the pioneering work by Goyder (1980). In the neighborhood of the *r-th* resonance, the inertance $H_{ij}(\omega)$ can be regarded as the sum of two terms:

$$H_{ij}(\omega) = \frac{-\omega^2 \Phi_{ir}\Phi_{rj}}{\omega_r^2 - \omega^2 + 2i\zeta_r\omega_r\omega} + \sum_{s\neq r=1}^{N} \frac{-\omega^2 \Phi_{is}\Phi_{js}}{\omega_s^2 - \omega^2 + 2i\zeta_s\omega_s\omega}. \tag{4.1}$$

The former is the prevailing resonant term and the latter is the contribution of all the other modes. By comparing the experimental (e) and the analytical inertance functions the error at the generic frequency ω_k around ω_r can be defined:

$$E_k = H_{ij}(\omega_k) - H_{ij}^{(e)}(\omega_k) = \frac{-\omega_k^2 \Phi_{ir}\Phi_{jr}}{\omega_r^2 - \omega_k^2 + 2i\zeta_r\omega_r\omega_k} - C_k \tag{4.2}$$

where the constant C_k is given by the difference between the experimental value of the FRF and the modal contributions of all the other modes $s \neq r$. By introducing the following modal quantities as variables of the problem:

$$a_r = \omega_r^2, \quad b_r = 2\zeta_r\omega_r, \quad c_{ijr} = \phi_{ir}\phi_{jr} \tag{4.3}$$

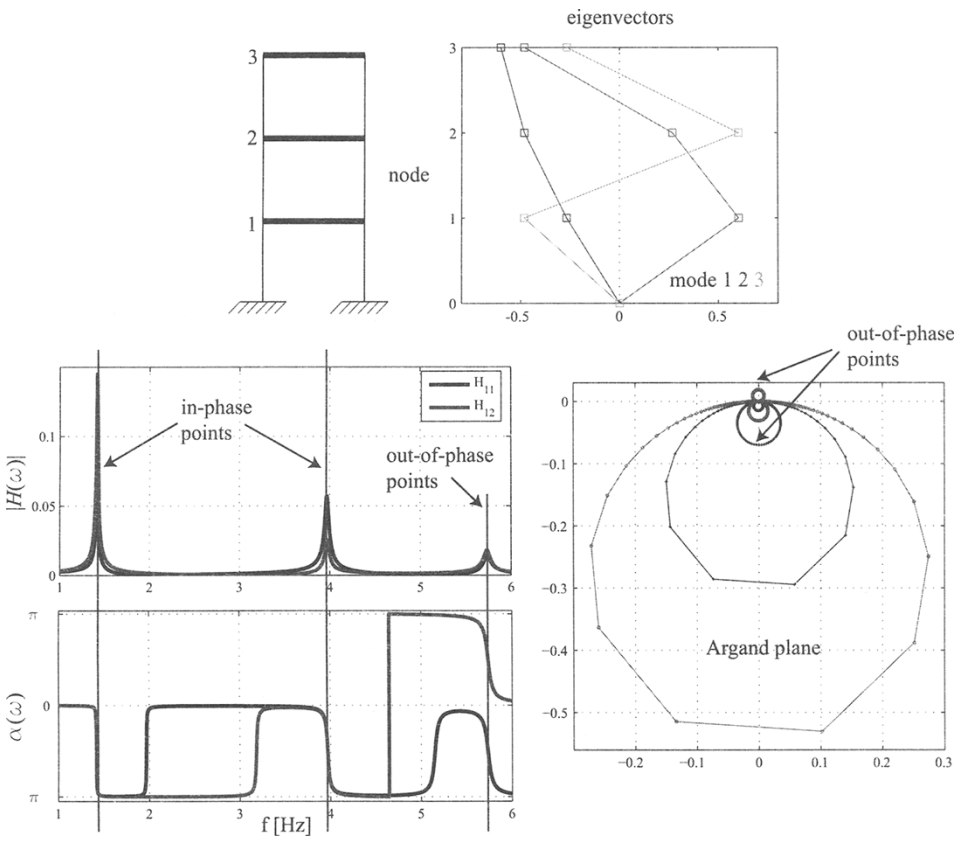

Figure 7. Display of the FRF H_{33} of a 3DOF system.

and a suitable weight function

$$w_k = \frac{-1}{a_r - \omega_k^2 + ib_r\omega_k}, \tag{4.4}$$

the error function can be linearized with respect to the assumed variables:

$$E_k = \frac{-\omega_k^2 \Phi_{ir}\Phi_{jr}}{\omega_r^2 - \omega_k^2 + 2i\zeta_r\omega_r\omega_k} - C_k = \omega_k^2 w_k c_{ijr} + w_k C_k \left(a_r - \omega_k^2 + ib_r\omega_k\right). \tag{4.5}$$

The procedure follows an iterative scheme: at the *h-th* iteration, the error is expressed as:

$$E_{k,h} = \omega_k^2 w_{k,h-1} c_{ijr,h} + w_{k,h-1} C_{k,h-1} \left(a_{r,h} - \omega_k^2 + ib_{r,h}\omega_k\right) \tag{4.6}$$

which is linear with respect to the three *r-th* modal unknowns since w_k and C_k are determined by the values at the step $h-1$. The objective function is obtained by summing the square error in a frequency range in the neighborhood of ω_r. On the basis

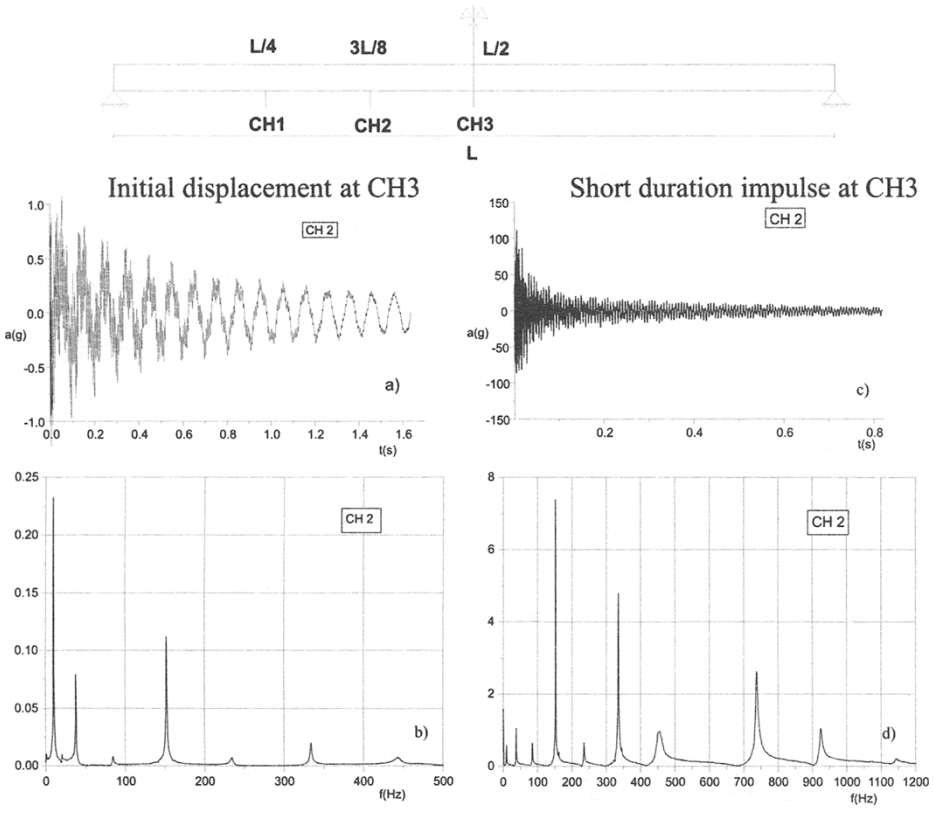

Figure 8. Free response and FRF of a simply supported beam.

of the least-squares method, the modal unknowns are determined. At each step, this procedure is extended to all meaningful resonances which appear in the response and, at the end of the process, all the modal parameters in the range of frequencies investigated are determined (Beolchini and Vestroni, 1994; Genovese and Vestroni, 1998; De Sortis et al., 2005).

The second method presented is a frequency domain decomposition method and relies on the response to ambient excitation sources when the output only is available. The method is based on the singular value decomposition of the spectral matrix (Brincker et al., 2001). It exploits the relationship:

$$\mathbf{G}yy\,(\omega) = \bar{\mathbf{H}}\,(\omega)\,\mathbf{G}xx\,(\omega)\,\mathbf{H}^{T}\,(\omega) \tag{4.7}$$

where $\mathbf{G}xx(\omega)$ (RxR, R number of inputs) and $\mathbf{G}yy(\omega)$ (MxM, M number of measured responses) are respectively the input and output power spectral density matrices, and $\mathbf{H}(\omega)$ is the frequency response function matrix (MxR).

Supposing the inputs at the different points to be completely uncorrelated and white

noise, $\mathbf{G}xx$ is a constant diagonal matrix $\mathbf{G}$, independent of ω. Thus:

$$\mathbf{G}yy\,(\omega) = G\,\mathbf{H}\,(\omega)\,\mathbf{H}^T\,(\omega) \tag{4.8}$$

whose term jk can be written as, by omitting the constant G:

$$Gyy_{jk}\,(\omega) = \sum_{r=1}^{R}\left(\sum_{p=1}^{N}\frac{\phi_{jp}\phi_{rp}}{\bar{\lambda}_p^2-\omega^2}\right)\left(\sum_{q=1}^{N}\frac{\phi_{kq}\phi_{rq}}{\lambda_q^2-\omega^2}\right). \tag{4.9}$$

In the neighborhood of the *i-th* resonance, the previous equation can be written as:

$$Gyy_{jk}\,(\omega) \cong \sum_{r=1}^{R}\frac{\phi_{ji}\phi_{ri}}{\bar{\lambda}_i^2-\omega^2}\frac{\phi_{ki}\phi_{ri}}{\lambda_i^2-\omega^2} = \frac{\phi_{ji}\phi_{ki}}{\left(\bar{\lambda}_i^2-\omega^2\right)\left(\lambda_i^2-\omega^2\right)}\sum_{r=1}^{R}\phi_{ri}^2 \tag{4.10}$$

where $\sum_{r=1}^{R}\phi_{ri}^2$ is a constant. By ignoring this term, the matrix $\mathbf{G}yy$ can thus be expressed as the product of three matrices:

$$\mathbf{G}yy\,(\omega) = \mathbf{\Phi}\mathbf{\Lambda}_i\mathbf{\Phi}^T \tag{4.11}$$

which represents a singular value decomposition of the matrix $\mathbf{G}yy$, where:

$$\mathbf{\Lambda}_i = \begin{bmatrix} \frac{1}{\left(\lambda_i^2-\omega^2\right)\left(\bar{\lambda}_i^2-\omega^2\right)} & 0\ldots & 0 \\ 0 & 0\ldots & 0 \\ 0 & 0\ldots & 0 \end{bmatrix}. \tag{4.12}$$

The peaks of the first singular values indicate the natural frequencies of the system. In the neighborhood of the *i-th* peak of the first singular value, the first singular vector is coincident with the *i-th* eigenvector. This occurs at each *j-th* resonance, when the prevailing contribution is given by the *j-th* mode. This procedure, which had recently a great diffusion, was implemented in a commercial code (ARTeMIS).

5 Conclusions

For SDOF and NDOF systems the knowledge of $H(\omega)$ provides a predictive model of the mechanical system in evaluating the response to any excitation. Moreover, it is possible to obtain experimental values of some components of $H(\omega)$ and then extract experimental values of modal parameters which are characteristic dynamic properties of the structure. Several methods in frequency and time domain are available to evaluate modal parameters from measured response to known and unknown excitation.

Bibliography

ARTeMIS. *modal software, www.svibs.com.*

G. C. Beolchini and F. Vestroni. Identification of dynamic characteristics of base-isolated and conventional buildings. In *Proceedings of the 10th European Conference on Earthquake Engineering*, 1994.

S. Braun, D. Ewins, and S. S. Rao, editors. *Encyclopedia of Vibration*, 2001. Academic Press, San Diego.

R. Brincker, L. Zhang, and P. Andersen. Modal identification of output-only systems using frequency domain decomposition. *Smart Materials and Structures*, 10:441–445, 2001.

R. R. Craig. *Structural Dynamics.* John Wiley & Sons, 1981.

A. De Sortis, E. Antonacci, and F. Vestroni. Dynamic identification of a masonry building using forced vibration tests. *Engineering Structures*, 27:155–165, 2005.

D. J. Ewins. *Modal Testing: theory, practice and application.* Reaserch Studies Press, 2000.

F. Genovese and F. Vestroni. Identification of dynamic characteristics of a masonry building. In *Proceedings of the 1th European Conference on Earthquake Engineering*, 1998.

H. G. D. Goyder. Methods and applications of structural modelling from measured frequency response data. *Journal of Sound and Vibration*, 68:209–230, 1980.

N.M.M. Maia and J.M.N. Silva. *Theoretical and Experimental Modal Analysis.* Reaserch Studies Press, 1997.

L. Meirovitch. *Principles and Techniques of Vibration.* Prentice-Hall, 1997.

Damage Identification using Inverse Methods

Michael I. Friswell
Department of Aerospace Engineering, University of Bristol, Bristol BS8 1TR, UK.
m.i.friswell@bristol.ac.uk

Abstract This chapter gives an overview of the use of inverse methods in damage detection and location, using measured vibration data. Inverse problems require the use of a model and the identification of uncertain parameters of this model. Damage is often local in nature and although the effect of the loss of stiffness may require only a small number of parameters, the lack of knowledge of the location means that a large number of candidate parameters must be included. This leads to potential ill-conditioning problems, and this topic is reviewed in this chapter. This chapter then goes on to discuss a number of problems that exist with the inverse approach to structural health monitoring, including modelling errors, environmental effects, damage localisation, regularisation, models of damage and sensor validation.

1 Introduction to Inverse Methods

Inverse methods combine an initial model of the structure and measured data to improve the model or test an hypothesis. In practice the model is based on finite element analysis and the measurements are acceleration and force data, often in the form of a modal database, although frequency response function (FRF) data may also be used. The estimation techniques are often based on the methods of model updating, which have had some success in improving models and understanding the underlying dynamics, especially for joints (Friswell and Mottershead, 1995; Mottershead and Friswell, 1993). Model updating methods may be classified as sensitivity or direct methods. Sensitivity type methods rely on a parametric model of the structure and the minimisation of some penalty function based on the error between the measured data and the predictions from the model. These methods offer a wide range of parameters to update that have physical meaning and allow a degree of control over the optimisation process. The alternative is direct updating methods that change complete mass and/or stiffness matrices, although the updated models obtained are often difficult to interpret for health monitoring applications. These methods will be considered in more detail later. However it should be emphasised that a huge number of papers have been written on the application of inverse methods to damage identification, and this chapter aims to give an overview of the approaches rather than a complete literature review. This chapter will also consider some of the difficulties that occur when inverse methods are used for damage identification (Friswell, 2007; Doebling et al., 1998).

The four stages of damage estimation, first given by Rytter (1993), are now well established as detection, location, quantification and prognosis. Detection is readily

performed by pattern recognition methods or novelty detection (Worden, 1997; Worden et al., 2000). The key issue for inverse methods is location, which is equivalent to error localisation in model updating. Once the damage is located, it may be parameterised with a limited set of parameters and quantification, in terms of the local change in stiffness, is readily estimated. Prognosis requires that the underlying damage mechanism is determined, which may be possible using inverse methods using hypothesis testing among several candidate mechanisms. This questions is considered in more detail later in the chapter. However, once the damage mechanism is determined, the associated model is available for prognosis, and this is a great advantage of model based inverse methods.

1.1 Objective Functions

Friswell and Mottershead (1995) discussed sensitivity based methods in detail. The approach minimises the difference between modal quantities (usually natural frequencies and less often mode shapes) of the measured data and model predictions. This problem may be expressed as the minimization of J, where

$$J(\theta) = \|\mathbf{z}_m - \mathbf{z}(\theta)\|^2 = \epsilon^T \epsilon \tag{1.1}$$

and

$$\epsilon = \mathbf{z}_m - \mathbf{z}(\theta). \tag{1.2}$$

Here $\mathbf{z}_m$ and $\mathbf{z}(\theta)$ are the measured and computed modal vectors, θ is a vector of all unknown parameters, and ϵ is the modal residual vector. The modal vectors may consist of both natural frequencies and mode shapes, although often mode shapes are only used to pair individual modes. If mode shapes are included then they must be carefully normalised, the sensor locations must be carefuly matched to the finite element degrees of freedom and weighting should be applied to Equation (1.1).

Frequency response functions may also be used, although a model of damping is required, and the penalty function is often a very complicated function of the parameters with many local minima, making the optimisation very difficult. dos Santos et al. (2005) presents an example of such a method for damage in a composite structure.

1.2 Sensitivity Methods

Sensitivity based methods allow a wide choice of physically meaningful parameters and these advantages has led to their widespread use in model updating. The approach is very general and relies on minimising a penalty function, which usually consists of the error between the measured quantities and the corresponding predictions from the model. Parameters are then chosen that are assumed uncertain, and these are usually estimated by approximating the penalty function using a truncated Taylor series and iterating to obtain a converged solution. If there are sufficient measurements and a restricted set of parameters then the identification may be well-conditioned. Often some form of regularisation must be applied, and this is considered in detail later. Other optimisation methods may be used, such as quadratic programming, simulated annealing or genetic algorithms, but these are not considered further in this chapter. Problems will also arise